Remote sensing of solar-induced chlorophyll fluorescence for describing photosynthesis seasonality in the Amazon forest

Gabriel Bertani [1]
Liana O. Anderson [1,2]
Luiz E.O.C. Aragão [1]
Fabien H. Wagner [1]

[1] Tropical Ecosystems and Environmental Sciences Group (TREES)
National Institute for Space Research – INPE
São José dos Campos 12227-010, SP, Brazil
{gabrielb, laragao}@dsr.inpe.br
fabien.wagner@inpe.br

[2] National Center for Monitoring and Early Warning of Natural Disasters - CEMADEN
São José dos Campos 12247-016, SP, Brazil
liana.anderson@cemaden.gov.br

Abstract. Recently, a new way of studying photosynthesis by remote sensing have been discovered, through the solar induced CHolorophyll Fluorescence (ChlF). In this paper, we review the main concepts and mechanisms used to retrieve ChlF by remote sensing. This includes space-based approaches, whose ChlF retrieval is more difficult to be achieved mainly due to atmospheric and sensors limitation issues, that can be mitigated with the launch of the FLEX mission. In addition, a set of ChlF data from the Gome-2 sensor and incident radiation reanalysis data from GLDAS, spanning the 2007-2015 period, were used to analyze the relationship between photosynthesis and radiation seasonality in the Amazon forest by decomposing the original data through the BFAST algorithm. The maximum incident radiation is observed from August to October in most part of the Amazon forest. On the other hand, the maximum photosynthesis activity occurs mainly from September to December. The photosynthetic activity increased after incident radiation raised, with a time-lag varying from one to three months, potentially related to the production of new leaves after the vegetation perceived the increase in the radiation signal. Photosynthesis seasonality thus varies spatially and seems to have a strong relation with radiation signals in the Amazon forest.

Key-words: solar-induced chlorophyll fluorescence, remote sensing, amazon forest, photosynthesis seasonality.

1. Introduction

The photosynthesis analysis of the Amazon rainforest is of primary importance because it is the largest tropical forest and represents 14% of all carbon fixed by photosynthesis in the terrestrial biosphere (Zhao and Running, 2010). In remote sensing studies, the potential photosynthetic rates of vegetation are usually modeled from reflectance data in the form of vegetation indices, which are basically values obtained by combining different spectral channels. However, photosynthesis is an actively regulated process with its efficiency highly variable. The plants can rearrange or alter pigments concentration in the leaves in order to adjust to prevailing environmental conditions, without any detectable changes in their reflectance properties (Meroni et al., 2009). In addition, vegetation indices may saturate in forest areas and have values changing depending on the sensor acquisition geometry (Morton 2014 et al.; Galvão et al., 2013). An alternative to this approach is the solar-induced Chlorophyll fluorescence (ChlF), which consists in radiation emitted by plants between 650 and 800 nm after energy absorption. Unlike reflectance based values, ChlF consists of a dimensional variable, providing a direct approach measurement of the functional status of vegetation, without the saturation in dense forests and sun/sensor geometry artefacts constraints inherent of vegetation indices.

Space-based observations of ChlF have been made through sensors in satellite missions designed to study atmospheric components, such as the Global Ozone Monitoring

Experiment-2 (Gome-2) and the Thermal and Near Infrared Sensor for Carbon Observation Fourier-Transform Spectrometer (TANSO-FTS), as they feature high spectral resolution spectrometers that encompass the spectral range of ChlF and a high Signal-to-Noise ratio. However, space-based observation of ChlF is still challenging and the mechanisms used to retrieve this variable are not trivial (Frankenberg et al., 2010). Besides that, space-based ChlF retrieval is a novel field of study, what makes this topic unheralded in the scientific community.

Several methods for ChlF retrieval have been proposed and some attempts succeeded to relate ChlF with the functional status of vegetation and carbon flux balance (Meroni et al., 2009). The strong ChlF / photosynthesis relationship (Porcar-Castell et al., 2014) and good results obtained by space-based retrievals of ChlF (Guanter et al., 2010; Joiner et al., 2013) makes this variable an alternative to vegetation indices applied to analyze photosynthesis seasonality in the Amazon forest (Guan et al., 2015; Wagner et al., 2016). In the amazon evergreen forest, the ecosystem photosynthesis is increased in response to radiation, when younger and more light-use efficient leaves grows (Wu at al., 2016). However, the spatial variation of the photosynthesis seasonality and its responses to radiation signal are not well understood in this region.

In this paper, we first review the main concepts and mechanisms used to obtain ChlF. Subsequently, we analyzed the relation between radiation and ChlF seasonality, used here as a proxy for the vegetation photosynthetic activity. ChlF and radiation data were decomposed to obtain their seasonality components, in order to determine the periods of maximum photosynthesis and the spatial distribution of its responses to radiation signal.

2. Concepts Review

The energy absorbed by chlorophyll molecules of a plant (photosynthetically active radiation - PAR, in the 400-700 nm wavelength region) has three destinations: (i) it can be used in photosynthesis, (ii) dissipated as heat (non-photochemical quenching) or (iii) re-emitted in the form of radiation as ChlF (Maxwell and Johnson, 2000). In this process, the radiation is re-emitted at longer wavelengths (fluorescence) between 660 to 800nm, with two emission peaks near to 690 and 740 nm (Meroni et al., 2009).

Assuming that fluorescence and reflectance of the surface follows the Lambert law, radiance from the direction of the vegetation to the sensor (L) is composed by the reflected energy from the surface (rE / π) and the emitted energy (F) (Meroni et al, 2009):

$$L(\lambda) = \frac{r(\lambda)E(\lambda)}{\pi} + F(\lambda)\ [Wm^{-2}sr^{-1}\mu m^{-1}] \quad (1)$$

λ = wavelength, r = reflectance, E = total incident irradiance

The reflectance factor (r) is obtained by the ratio between the radiation that reaches the sensor and the incident flow. However, this ratio also encompasses the fluorescence contribution (F). The inclusion of (F) to the reflectance factor is nominated as apparent reflectance (r*):

$$r^*(\lambda) = \frac{\pi L(\lambda)}{E(\lambda)} = r(\lambda) + \frac{\pi F(\lambda)}{E(\lambda)} \quad (2)$$

Fluorescence contributes only with a small portion of the total apparent reflectance signal that reaches the sensor (composed also by the reflected radiation from the surface) - about 1 to 2% (Moreno, 2015). As the fluorescence is masked by the radiation reflected from vegetation, decomposing these signals is not trivial. To separate the small fluorescence signal from the reflected radiance, the current remote sensing techniques utilize dark features in the Earth's

reflected spectrum, represented by telluric absorption or solar Fraunhofer lines, where solar incident irradiance is reduced. Telluric absorption occurs in the O_2 - A (~760 nm) and O_2 - B (~690 nm) bands, where atmospheric molecular oxygen absorbs incoming solar light (incident radiation is attenuated up to more than 90%). The Fraunhofer lines consist of narrow absorption bands in the solar spectrum caused by the elements present in sun photosphere. Thus, the ratio of fluorescence by reflectance is higher in the absorption bands, since irradiance is significantly reduced.

2.1 ChlF estimation

Chlorophyll fluorescence is retrieved in physical units and isolated from the reflectance by applying methods based on radiance data. The Radiance-based methods exploits the dark absorption bands of the incident radiation to decouple ChlF from the reflected flux (Meroni et al, 2009). According to the spectral requirements, the radiance-based methods can be divided into multispectral and hyperspectral. While the former requires only two or three bands to decouple the fluorescence signal, the latter demands several bands to form a contiguous range of spectral data.

The first multispectral method proposed to retrieve ChlF was the Fraunhofer Line Depth – FLD (Plascyk and Gabriel, 1975), which all radiance-based approaches are derived from. This method utilizes two spectral channels, one inside and one near to a dark absorption band, and utilize four variables: solar irradiance (Figure 1.a) and target radiance (Figure 1.b), inside and outside a dark absorption band. Fluorescence and reflectance are considered constant inside and outside the absorption band.

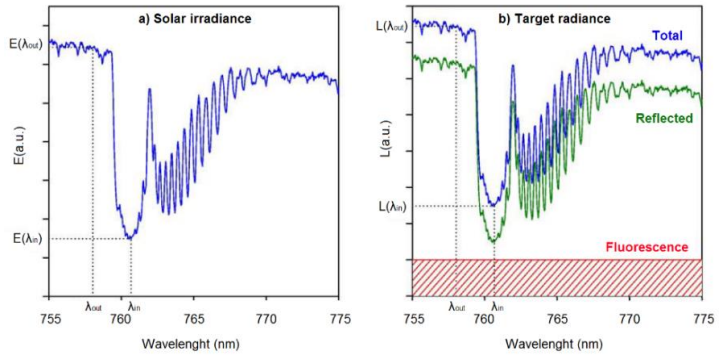

Figure 1. Fraunhofer Line Depth (FLD) principle depicted by measurements inside and outside the O_2-A band analyzed with a full-width-at-half-maximum - FWHM = 0.13 nm (Adapted from Meroni et al, 2009). a) Solar irradiance. b) Upwelling fluxes. The total upwelling flux is composed by the reflected and emitted (fluorescence) fluxes.

The incident (E) and upwelling (L) radiances are required in both spectral channels, to solve the system of equations:

$$L(\lambda_{in}) = \frac{r(\lambda_{in})E(\lambda_{in})}{\pi} + F(\lambda_{in}) \qquad L(\lambda_{out}) = \frac{r(\lambda_{out})E(\lambda_{out})}{\pi} + F(\lambda_{out}) \tag{3}$$

λin = signal measured inside the dark absorption band
λout = signal measured outside the dark absorption band

Assuming that reflectance (r) and fluorescence (F) are constant inside and outside the absorption band:

$$r = \frac{L(\lambda_{out}) - L(\lambda_{in})}{E(\lambda_{out}) - E(\lambda_{in})} + \pi \qquad F = \frac{E(\lambda_{out}) \times L(\lambda_{in}) - L(\lambda_{out}) \times E(\lambda_{in})}{E(\lambda_{out}) - E(\lambda_{in})} + \pi \tag{4}$$

However, the values of r and F are not constant inside and outside the absorption band (Alonso et al., 2008; Gómez-Chova et al., 2006). A hyperspectral approach was proposed to overcome this limitation: the improved FLD – iFLD method, that utilizes two correction

factors (αr for reflectance and αF for fluorescence) to consider the r and F variation inside and outside the absorption bands (Alonso et al., 2008). On the other hand, the Spectral Fitting Methods – SFM assume that there is a linear/quadratic variation of reflectance and fluorescence over the absorption bands. These methods utilize spectral fitting techniques based on linear/quadratic regression to retrieve F (Mazzoni et al., 2008; Guanter et al., 2009).

2.2 Space-based observations of ChlF

The use of Fraunhofer lines for fluorescence retrieval from space is difficult because their low spectral overlap with the peaks in the chlorophyll-a fluorescence emission spectrum. Absorption bands originated from water vapor features are discarded, because its high spatial and temporal variability (Guanter et al., 2010). Therefore, the space-based fluorescence retrieval is usually made by O_2 absorption lines. This approach works adequately near the surface, since atmospheric scattering can be neglected and the atmospheric effect on the irradiance can be normalized by using reference panels. However, in observations from space there is reabsorption of the fluorescence emission by O_2, in the path between the surface and the sensor. In the center of the O_2 absorption lines the fluorescence can be completely absorbed at the top-of-the-atmosphere (TOA). In addition, the scattering caused by aerosols and clouds causes an infilling in the absorption lines that is very similar to that caused by the fluorescence signal (Frankenberg et al., 2011).

In order to account for parameters affecting O_2 absorption, Guanter et al. (2010) used radiative transfer models over a simulated data set. They used the Matrix Operator MOdel - MOMO (Fell and Fischer, 2001) and the MODerate resolution atmospheric TRANsmission - MODTRAN4 (Berk et al., 2003) radiative transfer codes to generate aerosol scattering and surface pressure parameters. Others atmospheric parameters that may influence the O2-A and O2-B were not used in the simulation: thin and subpixel clouds, directional reflectance, temperature vertical profiles, polarization, water vapor, ring effect and dayglow emissions. The authors justified the omission of these parameters by considering them of second-order importance if compared to aerosol scattering and surface pressure. Besides, these factors can be accounted for by means of models or external data sources. Joiner et al. (2013) used global GOME-2 data combined with a radiative transfer model - MOMO (Fell and Fischer, 2001) - to disentangle the spectral signatures of three components: atmospheric absorption, surface reflectance, and fluorescence. A principal component analysis - PCA was applied to model the atmospheric absorption. The fluorescence information retrieved by this methodology reached good precision and accuracy.

2.3 Feasibility of using orbital sensors for ChlF retrieval

No operational satellite mission was planned specifically for obtaining ChlF. However, the evolution of the remote sensors that occurred in recent years, especially in term of the spectral resolution, allowed space-based ChlF analysis. This is the case of the current sensors TANSO-FTS and GOME-2. The TANSO-FTS is part of the Greenhouse gases Observing SATellite (GOSAT) that retrieves data on infrared light reflected and emitted from the earth's surface and the atmosphere. Band 1 of this sensor can be used to retrieve ChlF, with spectral coverage ranging from 758 – 775nm and spectral resolution equal to 0,27nm (Kuze et al., 2009). GOME-2 measures the Earth's backscattered radiance and the extraterrestrial solar irradiance at wavelengths between 240 and 790 nm in four spectral bands. Band 4 of this sensor can be used to retrieve chlorophyll fluorescence, with spectral coverage ranging from 590–790nm and spectral resolution of 0,5nm (Callies et al., 2000). It's worth to observe the trade-off between spectral and spatial resolutions on ChlF retrieval. While a higher spectral resolution permits more accurate ChlF retrievals, this feature sacrifices the spatial sampling (Frankenberg et al., 2014). Chfl generated from TANSO-FTS observations are better

characterized but the spatial resolution is coarser. Generally, GOME-2 based approaches obtain ChlF with ground-pixels equivalent to 0.5° (Joiner et al., 2013), while ChlF retrieved from TANSO-FTS has ground-pixels equivalent to 2° (Köhler et al., 2015). Limitations inherent to current satellite ChlF acquisition mechanisms can be mitigated with the launch of the FLEX mission. The FLEX was developed specifically for obtaining ChlF on a global scale through the Fluorescence Imaging Spectrometer - FLORIS, which has a spatial resolution of 300m and a swath of 150 km. This instrument uses two imagers spectrometers combined for measuring the radiance between 500 and 780 nm, with a spectral resolution of 0.3 nm. It comprises the entire chlorophyll fluorescence spectrum, the Oxygen A (755-780 nm) and Oxygen B (677-697 nm) bands. This instrument will also acquire the photochemical reflectance (500-600 nm), chlorophyll absorption (600-677 nm) and near infrared (697-755 nm) spectra as well. Still, this satellite will be in formation with Sentinel-3, which will subsidize the characterization of the atmosphere and the presence of clouds at the time of acquisition (Moreno, 2015).

3. Material and Methods

3.1 Datasets

ChlF seasonality was used here as a proxy for the vegetation photosynthetic activity in Amazon. We assume that when ChlF increases there is production of new leaves, as occur with the Enhanced Vegetation Index – EVI (Wu et al., 2016). The Chlf data covering the Amazon forest was obtained from the monthly GOME2_F product - level 3 version 26 (V26) (Joiner et al., 2016), obtained in a window with wavelengths between 734 and 758 nm, for the 2007-2015 period. The spatial resolution of GOME2_F corresponds to 0. 5°. Radiation data were obtained by reanalysis products from the Global Land Data Assimilation System (GLDAS) (Rodell et al., 2004). The GLDAS product used in this paper correspond to monthly incoming shortwave radiation - Version 1, which has a spatial resolution of 0.25° and is generated with the Noah Land Surface Model (Koren et al., 1999). We used the treecover2000 and Global forest cover loss from 2000 to 2014 products to define the forest regions in the study area, both obtained from the Global Forest Change Project 2000-2014 – GFCP (Hansen et al., 2013). All products of this project have a spatial resolution of 30 meters. The global forest cover loss product 2000-2014 represents the deforested areas between 2000-2014.

3.2 Processing

a) A mask representing deforested pixels, obtained from the Global forest cover loss 2000-2014 product, was applied over the treecover2000 data, to make the values defined as forest in 2000 and were cleared until the end of 2014 equal to zero. b) Radiation and treecover2000 data were resampled to a spatial resolution of 0.5 ° - the same of the ChlF data. These new values were defined by averaging the original pixels from radiation and treecover2000 contained in a 0.5° x 0.5° grid (resampled treecover2000 results in a proportion of forested areas for each pixel). c) A mask of the resampled treecover2000 product containing only pixels with forest cover equal or greater than 70% were applied in all data sets. Therefore, the analysis presented in this study refers only to evergreen forests. d) ChlF and GLDAS monthly seasonality were extracted by the Breaks in Additive Season and Trend - BFAST algorithm. This algorithm is well described in Verbesselt et al. (2010). e) ChlF and radiation monthly seasonality maximum peaks were compared. This way, one, two or three lag months were applied to radiation data, to investigate when photosynthesis increases in response to radiation.

4. Results

The maximum photosynthesis occurs mainly between September and December, in 87,54% of the Amazon forest (Figure 2.A). While areas where the maximum photosynthesis occurs in November are more dispersed, areas which maximum photosynthesis occurs in December and September were concentrated in the southern and northern Amazon, respectively. The epicenter of the maximum photosynthesis peaking in October are concentrated mainly in the north-east amazon. On the other hand, maximum incident radiation peaks occur in a narrow time-window if compared to the photosynthesis, between August and October, in 92.9% of the Amazon forest - mainly in September - 78.71% (Figure 2.B). Contrary to photosynthesis, the radiation monthly peaks are more concentrated. Areas which maximum radiation occurs in September are present in most part of Amazon, while areas where maximum radiation occurs in August and October are located in the eastern and western parts, respectively.

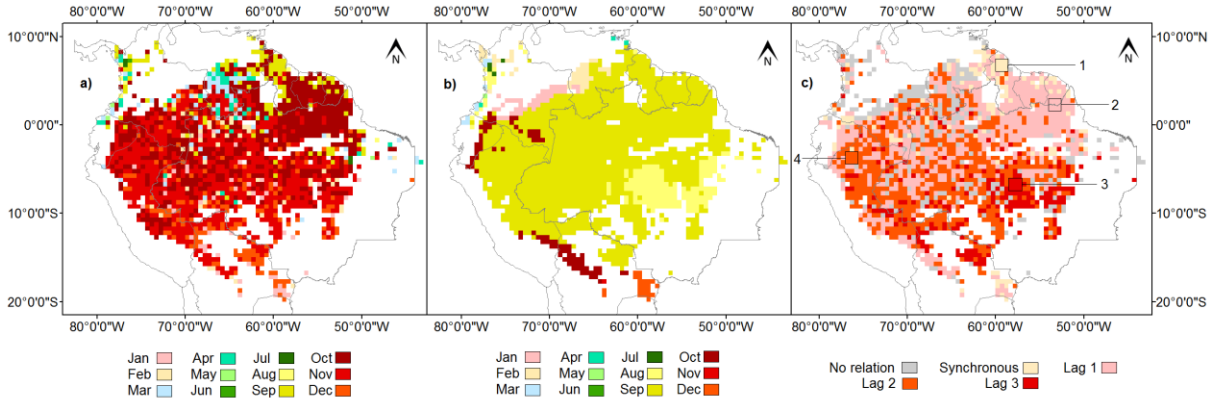

Figure 2. Spatial patterns of maximum photosynthesis (a) and (b) maximum radiation seasonality. c) Lags observed between maximum photosynthesis and radiation. Highlighted regions indicate areas where mean seasonality was obtained.

In 7.5% of the Amazon forest the maximum photosynthesis monthly peak was synchronous with the incident radiation, while in 90,22% there was at least one month lag between the photosynthesis and radiation peaks (Figure 2. C). Synchronicity between photosynthesis and radiation occurred mainly in northern Amazonia. One-month-lag was observed over almost all Amazon, with the exception of the south-east region. These areas were more concentrated in the north-east region. Two-month-lag areas were broadly distributed too, with the exception to the north-east region, where only a few areas were observed. Three-month-lag areas occurred mainly in the southern region. Mean seasonality of the highlighted regions in Figure 2. C (1, 2, 3 and 4) are showed in the Figure 3.

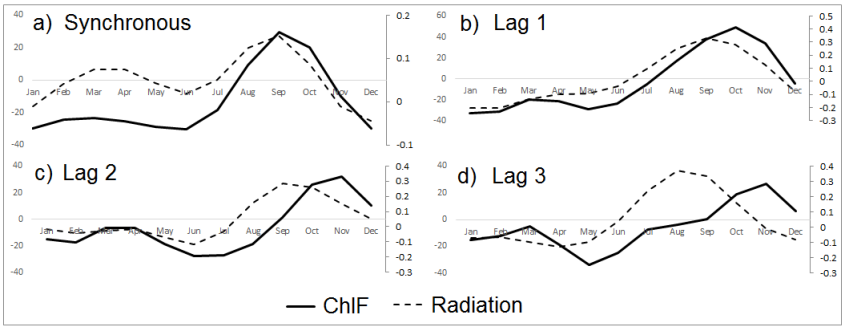

Figure 3. a) Mean seasonality of regions where there is synchronicity between the seasonal maxima of photosynthesis and radiation. Figures b), c) and d) show the mean seasonality of regions where there is a time lag (in months) between the seasonal maxima of photosynthesis and radiation.

The lags observed between the photosynthesis and radiation peaks are likely explained by a perception of the vegetation when the radiation signal increases (Restrepo-Coupe et al., 2013) (Figure 3). The buds are not present on vegetation during the wet season in the Amazon forest, when the radiation signal is low, but as insolation increases they are developed and the production of new leaves occurs (Klebs, 1914; Borchert et al., 2015). We didn't analyze the sensitivity of the vegetation to water in precipitation limited areas. In such areas, the photosynthesis signal is more influenced by precipitation, and represents the vegetation sensibility to detect the shifting from drought to wet season (Borchert, 1994).

5. Conclusions

- Decoupling of ChlF from the reflected signal and its atmospheric components is still challenging.
- The FLEX can help to solve issues such as the atmospheric influence over the radiance signal and the gross spatial resolution of the current sensors used to obtain ChlF.
- Photosynthesis seasonality tends to be higher from September to December in the most part of the Amazon forest.
- Most part of the maximum photosynthesis occurs between one to three months after the peaks in radiation seasonality in the Amazon forest.

Acknowledgments

We gratefully acknowledge the CAPES and FAPESP (Grants No. 13/14520-6 and No. 2013/50533-5) agencies for providing research fellowships and support this work.

References

Alonso, L.; Gómez-Chova, L.; Vila-Francés, J.; Amorós-López, J.; Guanter, L.; Calpe, J., et al. Improved Fraunhofer Line Discrimination method for vegetation fluorescence quantification. **IEEE Geoscience and Remote Sensing Letters**, v.4, p. 620–624, 2008.

Berk, A.; Anderson, G. P.; Acharya, P. K.; Hoke, M. L.; Chetwynd, J. H.; Bernstein, L. S.; Shettle, E. P.; Matthew, M. W.; S. M., MODTRAN4 Version 3 Revision 1 user's manual, **Air Force Res. Lab.**, 2003.

Borchert, R., Calle, Z.; Strahler, A. H.; Baertschi, A.; Magill, R. E.; Broadhead, J. S; Kamau, J.; Njoroge, J.; Muthuri, C. Insolation and photoperiodic control of tree development near the equator, **New Phytologist,** v. 205, n. 1, p. 7–13, 2015.

Brienen, R. J. W. et al. Long-term decline of the Amazon carbon sink, **Nature**, v. 519, n. 7543, p. 344–348, 2015.

Fell, F.; Fischer, J. Numerical simulation of the light field in the atmosphere–ocean system using the matrix–operator method, **J. Quant. Spectrosc. Ra.**, n. 69, p. 351–388, 2001.

Frankenberg, C.; Butz, A.; Toon, G. C. Disentangling chlorophyll fluorescence from atmospheric scattering effects in O2 A-band spectra of reflected sun-light, **Geophys. Res. Lett.**, n. 38, 2010.

Frankenberg, C.; Butz, A.; Toon, G. C. Disentangling chlorophyll fluorescence from atmospheric scattering effects in O2 A-band spectra of reflected sun-light, **Geophys. Res. Lett.**, n. 38, 2011.

Frankenberg, C.; O'Dell, C.; Berry, J.; Guanter, L.; Joiner, J.; Köhler, P. et al. Prospects for chlorophyll fluorescence remote sensing from the Orbiting Carbon Observatory-2,**Remote Sensing of Environment**, p. 1-12, 2014.

Galvão, L. S. et al. View-illumination effects on hyperspectral vegetation indices in the Amazonian tropical forest, **International Journal of Applied Earth Observation and Geoinformation**, v. 21, n.1, p. 291–300, 2012.

Guan, K.; Pan, M.; Li, H.; Wolf, A.; Wu, J.; Medvigy, D.; Lyapustin, A. I. Photosynthetic seasonality of global tropical forests constrained by hydroclimate. **Nature Geoscience**, v. 8, p. 284-289, 2015.

Guanter, L.; Alonso, L.; Gómez-Chova, L.; Meroni, M.; Preusker, R.; Fischer, J.; Moreno, J. Developments for vegetation fluorescence retrieval from spaceborne highresolution spectrometry in the O2 A and O2-B absorption bands, **J. Geophys. Res.**, n. 115, 2010.

Guanter, L.; Segl, K.; Kaufmann, H.; Verhoef, W.; Gomez-Chova, L.; Alonso, L., et al. Atmospheric corrections for fluorescence signal retrieval. **Final Report ESA – ESTEC**, 2009.

Hansen, M. C.; Potapov, P. V.; Moore, R.; Hancher, M.; Turubanova, S. A.; Tyukavina, A.; Thau, D.; Stehman, S. V.; Goetz, S. J.; Loveland, T. R.; Kommareddy, A.; Egorov, A.; Chini, L.; Justice, C. O.; Townshend, J. R. G. High-Resolution Global Maps of 21st-Century Forest Cover Change. **Science**, p.850–53, 2013.

Joiner, J.; Guanter, L.; Lindstrot, R.; Voigt, M.; Vasilkov, A. P.; Middleton, E. M.; Huemmrich, K. F.; Yoshida, Y.; Frankenberg, C. Global monitoring of terrestrial chlorophyll fluorescence from moderate spectral resolution near-infrared satellite measurements: methodology, simulations, and application to GOME-2, **Atmos. Meas. Tech.**, v. 6, p. 2803-2823, 2013.

Joiner, J.; Yoshida, Y.; Guanter, L.; Middleton, E. M. New methods for retrieval of chlorophyll red fluorescence from hyper-spectral satellite instruments: simulations and application to GOME-2 and SCIAMACHY. **Atmos. Meas. Tech. Discuss.**, n. 387, in review, 2016.

Klebs, G. (1914), Über das Treiben der einheimischen Bäume, speziell der Buche, Abhandl. Heidelberger Akad. Wiss. (Math. Nat. Kl.), 3, 1–112.

Köhler, P.; Guanter, L.; Joiner, J. A linear method for the retrieval of sun-induced chlorophyll fluorescence from GOME-2 and SCIAMACHY data. **Atmos.Meas.Tech.Discuss**. v.8, p. 2589 -2608, 2015.

Koren, V.; Schaake, J.; Mitchell, K.; Duan, Q.Y.; Chen, F.; Baker, J. M. A parameterization of snowpack and frozen ground intended for NCEP weather and climate models, J. Geophys. Res. Atmos, n. 104, p. 19569–19585, 1999.

Kuze, A.; Suto, H.; Nakajima, M.; Hamazaki, T. Thermal and near infrared sensor for carbon observation Fourier-transform spectrometer on the Greenhouse Gases 5 Observing Satellite for greenhouse gases monitoring, **Appl. Optics**, v. 48, p. 6716–6733, 2009.

Maxwell, K.; G. N. Johnson, Chlorophyll fluorescence - a practical guide. **J.Exp.Bot.**, v. 51, n. 345, p. 659–668, 2000.

Mazzoni, M.; Falorni, P.; Del Bianco, S. Sun-induced fluorescence retrieval in the O2-B atmospheric absorption band. **Optics Express**, v. 16, p. 7014–7022, 2008.

Meroni, M.; Rossini, M.; Guanter, L.; Alonso, L.; Rascher, U.;Colombo, R.; Moreno, J. Remote sensing of solar-induced chlorophyll fluorescence: review of methods and applications, **Remote Sens. Environ**., n. 113, p. 2037–2051, 2009.

Morton D. C. et al. Amazon forests maintain consistent canopy structure and greenness during the dry season, **Nature**, n. 506, p.221–224, 2014.

Pan, Y. et al. A large and persistent carbon sink in the world's forests. **Science**, n. 333, p. 988-993, 2011.

Plascyk, J. A.; Gabriel, F. C. The Fraunhofer Line Discriminator MKII - An airborne instrument for precise and standardized ecological luminescence measurements. **IEEE Transaction on Instrumentation and Measurement**, n.24, p. 306–313, 1975.

Porcar-Castell A.; Tyystjärvi E.; Atherton J.; van der Tol C.; Flexas J.; Pfündel E.; Moreno J.; Frankenberg C.; Berry J.A. Linking chlorophyll-a fluorescence to photosynthesis for remote sensing applications: mechanisms and challenges, **Journal of Experimental Botany**, v. 65, p. 4065–4095, 2014.

Rodell, M.; Houser, P.R.; Jambor, U.E.A.; Gottschalck, J.; Mitchell, K.; Meng, C.J.; Arsenault, K.; Cosgrove, B.; Radakovich, J.; Bosilovich, M. et al. The global land data assimilation system. **Bull. Am. Meteorol. Soc.**, v. 3, p. 381–394, 2004.

Verbesselt, J. et al. Detecting trend and seasonal changes in satellite image time series. **Remote Sensing of Environment**, n. 1, v. 114, p. 106–115, 2010.

Wu, J.; Albert, L. P.; Lopes, A. P.; Restrepo-Coupe, N.; Hayek, M.; Wiedemann, K. T.; Guan, K.; Stark, S. C.; Christoffersen, B.; Prohaska, N.; Tavares, J. V.; Marostica, S.; Kobayashi, H.; Ferreira, M. L.; Campos, K. S.; Silva, R.; Brando, P. M.; Dye, D. G.; Huxman,T. E.; Huete, A. R.; Nelson, B. W. Nelson; Saleska, S. R. Leaf development and demography explain photosynthetic seasonality in amazon evergreen forests. **Science**, n. 351, 2016.

Zhao, M.; S. W. Running. Drought-Induced Reduction in Global. **Science**, v. 329, n. 5994, p. 940–943, 2010.